

Energy Management Research using Emulators of Renewable Generation and Loads

Richard Davies, Amir Fazeli, Sung Pil Oe, Mark Sumner, Mark Johnson, Edward Christopher

Electrical and Electronic Engineering, University of Nottingham, Nottingham, England

Abstract — A laboratory based microgrid test facility is described which uses emulation systems to represent a variety of renewable generation and load types. The emulation systems use real time data from a small housing estate and a 9kW wind turbine to provide a safe, versatile and realistic testbed for the development of energy management techniques for small communities. The paper describes the facility and also two control techniques for energy and power quality management within an energy community.

Keywords — Microgrid, renewables, emulator, energy management, unbalance compensation.

I. INTRODUCTION

Renewable energy has seen growth for decades although more significantly in recent years [1-4] and with its increase in deployment at household level, the traditional “centralized” approach to electricity distribution is challenged. Additionally, electrification of heat and transport is expected to increase in the near future which will result in significant increase in electricity demand. The expected demand growth will exceed the distribution network asset thermal and electrical capacities.

Microgrids [5] have a certain synergy with renewable energy systems (RES), due to the flexible installation options such as wind, solar, geothermal or biomass. A microgrid may offer benefits of a more secure supply or improved protection as well as less dependence on centrally generated energy which is often from fossil fuels [6, 7]. An alternative view is to consider “energy communities” - group of users such as a street, village, shopping mall or physical microgrid – where the community works together to manage energy consumption to achieve some benefit e.g. minimization of energy cost, reduction of peak current, maximization of local RES etc.

This paper introduces work undertaken to develop energy management for “communities”. The first section briefly introduces a specific energy community which will be the basis for testing the management algorithms developed. The second section then describes a laboratory test facility developed to emulate this community (allowing safer initial deployment of equipment and new algorithms) as well as being scalable to represent other types of energy community for hardware in the loop testing of new equipment and algorithms. The paper then goes on to describe the development and initial testing of algorithms for energy management and power quality enhancement within the microgrid facility.

II. THE CREATIVE ENERGY HOMES

The Creative Energy Homes (CEH) are a group of seven houses built specifically to research innovative state-of-the-art energy efficient homes though modern methods

of construction, energy efficient design and the use of RES. [8]. The houses contain instrumentation for monitoring and controlling electrical power usage and are occupied. Each house has a single phase supply and these are roughly balanced across a three phase supply which can be provided directly from the supply utility, or from a local 50kW generator which can be controlled to emulate frequency changes. These houses can be used as a test facility for new energy management strategies, for example demand side management, incorporation of energy storage etc. However, before deployment of any equipment within the CEH environment, it must be tested in a realistic laboratory environment which is described in the next section.

III. TEST FACILITY OVERVIEW

A 300kW microgrid test facility is being developed at the University of Nottingham to research and develop management and control strategies for microgrids, as well as providing a test facility for equipment developed for such environments. A key requirement of the test facility is to emulate a wide range of envisaged microgrid equipment, including renewable energy sources, energy storage devices and loads, for example electric vehicles, such that a microgrid’s behaviour can truly be created in real-time for the testing of proposed management algorithms and equipment.

The microgrid test facility comprises two, three phase distribution systems as shown in Fig. 1. The first is a 300kVA 50Hz 415V distribution system connected directly to the supply utility, which acts as the energy source and energy dump. The second is a variable frequency variable voltage distribution system (microgrid) which can either be fed from a motor generator system (with the motor driven through a variable speed drive), or can be supplied by emulated renewable energy systems (ERES).

The microgrid test facility will use real-time emulation of a wind turbine together with real time emulation of the CEH. The total electrical power fed to the houses is monitored at the distribution point, and can be communicated via a LAN or GPRS based communication system to the microgrid laboratory. The proposed test system is illustrated in Fig. 2. It shows the wind turbine communicating to the wind turbine emulator in the microgrid test facility. It also shows the data acquisition system at the Creative Energy Homes communicating with the microgrid test facility.

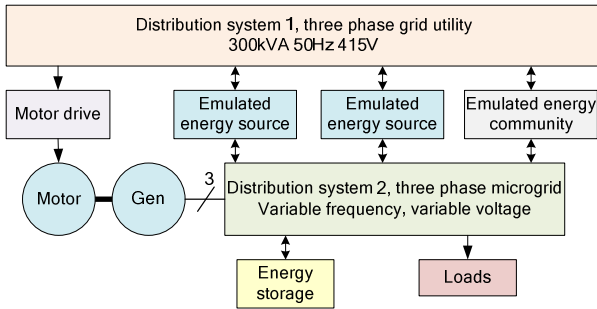


Fig. 1. Representation of the microgrid test facility.

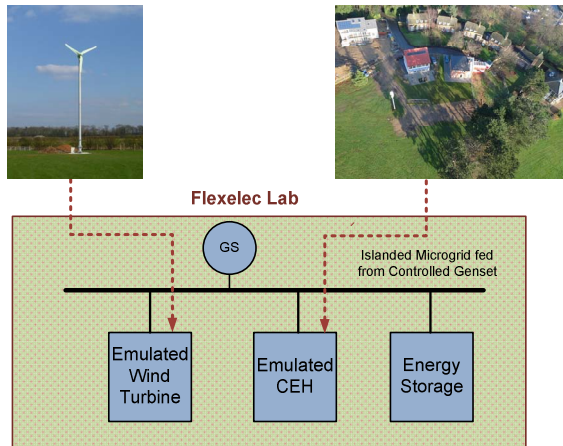


Fig. 2. Experimental Emulation of Energy Community

IV. EMULATION SYSTEMS

Each ERES is actually a four quadrant power electronic converter connected between the supply utility and the microgrid as shown in Fig. 3. The utility connection is created by an off-the-shelf commercial “active front end”, and requires only startup and shutdown signals. It automatically looks after power flow control based on the power it receives/supplies through its DC link. The microgrid connection on the other hand is a bespoke power converter connected at the DC link: it is programmed to act either as a current source or a voltage source, depend-

ing on its overall emulation characteristics. Commands for the real and reactive currents are obtained from a higher level controller running the emulation control.

For some emulated systems (for example a fuel cell) this control will be in the form of a pre-programmed algorithm derived from literature or from laboratory work. Alternatively the emulator can use data from the wind turbine or CEH community and can be applied in either of two ways. It can use the real-time data as a direct duplication of the installed systems creating a true representation of actual conditions. The second approach uses models and algorithms developed with simulations, in the case of the wind turbine with wind speed and direction data, to allow the power size to scale in a more sophisticated manner than a linear scaling of power data.

The ultimate aim is to continually telemeter measurements from the wind generator site to the microgrid test facility (using web based or GPRS communications) such that the wind emulator can be controlled continually in real time according to contemporaneous data from the real installation. This will be extremely useful for researching microgrid control algorithms that use, for example real-time web based weather forecasting or other available real-time data as part of their management strategy.

A 9kW wind turbine has been deployed at a rural location to provide data for a realistic wind turbine emulation system. The generator comprises horizontal axis 3 blade turbine with the rotational energy passed through a gear-box onto a cage induction machine generator. The drive system, two commercial power converters operating in back-to-back configuration, delivers the power from the variable speed generator to the grid, and incorporates filtering and protection to achieve G83 compliance. To maximize the energy capture the wind turbine has two degrees of control – generator speed control and active yaw control [9]. The control and data capture is implemented on a National Instruments CompactRIO. This is an expensive and complex processor but provides for flexibility and expansion if required. Fig. 4 shows a representation of wind turbine operational data received over a duration of three hours during testing.

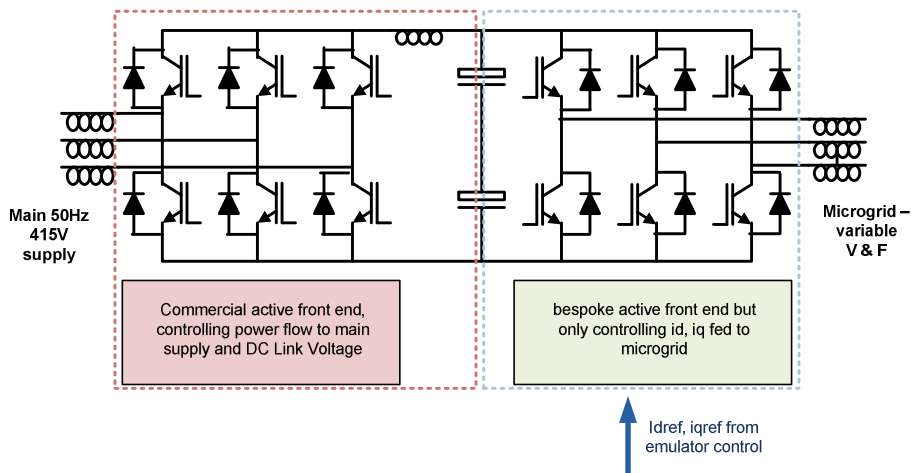


Fig. 3. Representation of emulation system connections

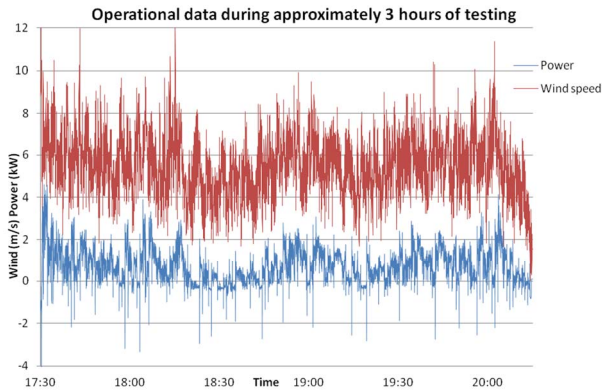


Fig. 4. Data from experimental operation of wind turbine.

V ENERGY MANAGEMENT IN THE CEH COMMUNITY

This section describes an approach to electrical energy management within the Creative Energy Homes community. The approach considers supplies and loads - Distributed Energy Resources (DER) - as different forms of dispatchable resources. For example the operation of elements such as combined heat and power (CHP), energy storage and loads with a thermal or electrical storage element can be moved forward in time. Load DERs commonly gain their dispatchability from their thermal/electrical storage element. Examples of such load DERs include thermal storage of a refrigerator and the battery of an electric vehicle.

It is envisaged that the incorporation of a suitable degree of intelligence for active management of DERs at different levels in the distribution network (such as the hierarchical structure presented in [10] and illustrated in Fig. 5) would facilitate the mass electrification of heat and transport; and the integration of stochastic renewable based generation units, without the need for major network asset replacement.

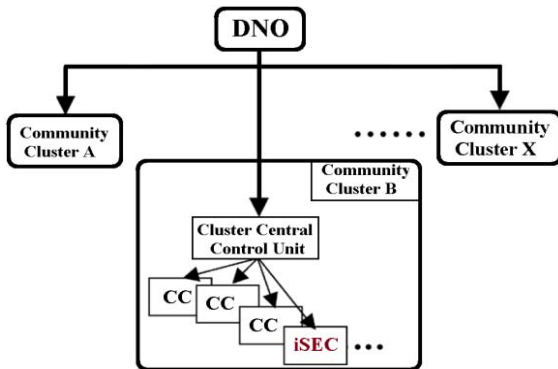


Fig. 5. Representation of loads

By applying the appropriate optimization technique at every level of the hierarchical structure, multiple objectives can be achieved at every level, which is expected to lead to both local and global optima across the entire distribution network (i.e. at the community cell and the DNO levels respectively). The optimization objectives at each level are different from other levels and include maximized use of renewable based generation, minimized network conduction losses and optimal operation of network assets, while all consumer needs are accommodated for. Forecasted renewable generation and forecasted demand are matched at the intermediate level of

the cluster of community cells and the top DNO level, whereas a deterministic optimization algorithm needs to determine operation of every participatory DER in real time in order to achieve a local objective function at the lowest level of community cell with an inherently unpredictable demand.

A deterministic optimization algorithm was designed and presented in detail in [10] which switches the required number of available DERs (i.e. seven refrigerators in this case) on and off in order to minimize the Community Power Flow (CPF) above a variable threshold (CPF_T). It was proposed that CPF_{PT} was received from one higher level within the hierarchical structure (i.e. cluster of community cells level), and is effectively the output of a probabilistic optimization algorithm at that level, which forms the connection between the community cell and the cluster of community cells levels.

CPF is quantified as the summation of the instantaneous demand, modeled using the bottom up approach presented in [11]. The distributed generation modeled including PV, a wind turbine, a μ CHP using the equation and method presented in [12-14] and a community battery energy storage model presented in [15].

The following objective function and constraints have been defined for the deterministic optimization algorithm which runs at real time and determines the number of required devices for dispatch (NRD).

$$\text{Min} \sum_{d=1}^{NRD} (CPF_{PT} - (NAD \times P_d)) \quad (1)$$

NAD is the number of available devices and P_d is the instantaneous power consumption of every participatory device d . The optimization algorithm runs at real time and is constrained by the minimum operating temperature of every participatory refrigerator.

A generation curtailment function (in the form of a search loop) is also incorporated as part of the DER optimal dispatch algorithm. The generation curtailment objective function is shown in “(2)”

$$\text{max} \sum_{g=1}^{NAG} (CPF - (NAG \times P_g)) \quad (2)$$

This function is initiated when CPF is negative (i.e. grid export operation) and less than CPF_T . In other words the instantaneous ideal grid export capacity is quantified by CPF_T and any power greater than CPF_T is curtailed. NAG is the number of available generation units and P_g the unit's instantaneous power generation for every participatory generation unit.

A. Simulation results

As illustrated in Fig. 6 by using the CPF_T received from the intermediate level cluster of community cells, resources are less frequently dispatched throughout the day. This in turn ensures that more resource thermal capacity is available for dispatch during the peak hours of the day (i.e. 2.9×10^4 s to 3.6×10^4 s and 7.5×10^4 s to 8.5×10^4 s) which results in more CPF reduction during these periods. This also results in less interruption for the consumer as the temperature of their refrigerator is regulated with their conventional thermostat function.

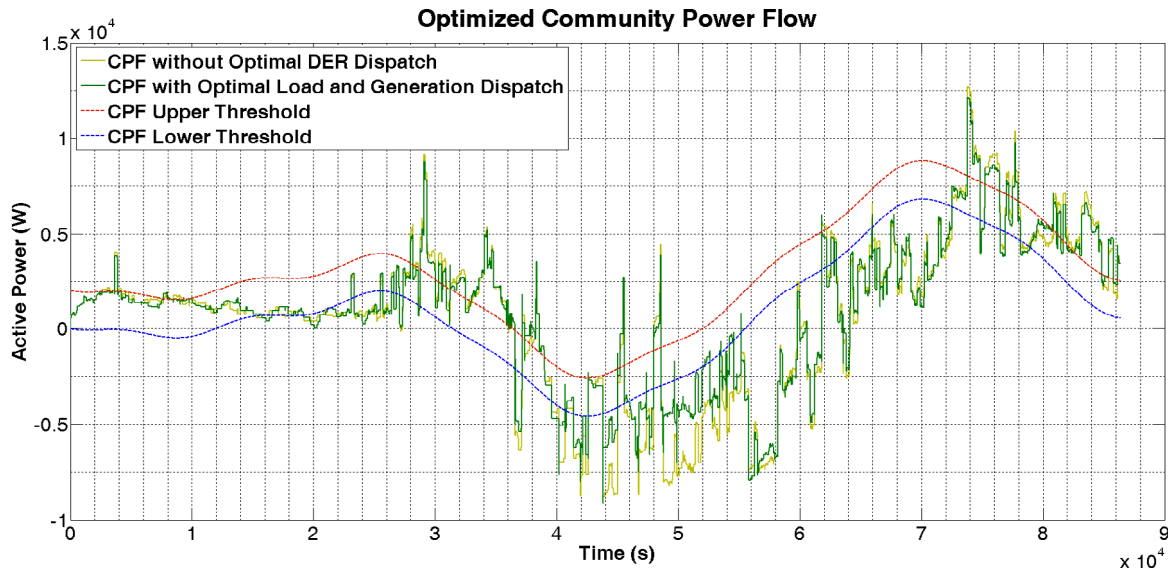


Fig. 6. CPF graph with optimal cold load dispatch with curve CPF threshold

The generation curtailment function is utilized during the mid-day peak generation hours between 4 and 5.6×10^4 s. The original value of CPF is negative and less than CPF_T and curtailment of two generation units (PV units of 2160W and 3120W generation capacity each) brings CPF closer and above the optimum solution of CPF_T .

By utilizing CPF_T signal in the local deterministic community optimization, a connection between different levels of the hierarchical system is established which ensures the effectiveness of the proposed hierarchical structure at reaching a quasi-optimal solution.

VI. COMPENSATION OF MICROGRID UNBALANCE

Due to the uneven distribution of loads across the 3 phases of a microgrid and their continuously varying demands, including single-phase micro-generation units, the Microgrid can operate under highly unbalanced conditions. Unbalanced loading leads to the flow of excessive neutral line currents, resulting in overloading of distribution feeders and transformers and can cause common mode noise which makes sensitive electronic equipment prone to malfunction [16]. Also, because the power system is inherently asymmetrical and the distribution feeder impedances are not equal across the 3 phases, voltage unbalance occurs. This will reduce the capacity of transformers, generate uncharacteristic harmonics and cause nuisance tripping of power electronic converters [17].

It is clear that unbalanced loading will cause technical problems to power system equipments but will also affect the safe and stable operation of the Microgrid. It is proposed that an unbalance compensating unit be connected in shunt at the point of common coupling (PCC), so that the Microgrid behaves as a model citizen from the viewpoint of the main grid. The Microgrid Unbalance Compensator (MUC) will detect and compensate the undesirable power components, improving balance and power quality of the Microgrid and will also limit its disturbance on the main grid.

A. MUC Structure

The main components of the MUC are the PWM Voltage Source Converter (VSC), the PWM current controller, DC voltage regulator and the compensation reference

current generator. Fig. 7 shows the schematic of the MUC.

A 3-phase four-leg IGBT-based VSC will be employed which will have the neutral line connected to the fourth leg. This configuration will allow the MUC to compensate the neutral current. The high-order harmonics at the switching frequency generated by the VSC can be filtered out by the passive filter shown in Fig. 7. The PWM current controller will force the output currents of the VSC to follow the reference currents hence the VSC connected through a coupling inductor will behave as a controlled current source. The role of the compensation reference current generator is to determine the current components needing to be compensated by the MUC. An additional component, \bar{P}_{loss} , determined from the DC voltage regulator will also be an input to the reference current generator. \bar{P}_{loss} represents the additional power required from the main supply to compensate the losses in the VSC. The DC voltage regulator controls the voltage across the capacitor, V_{DC} , to be regulated around a fixed reference value.

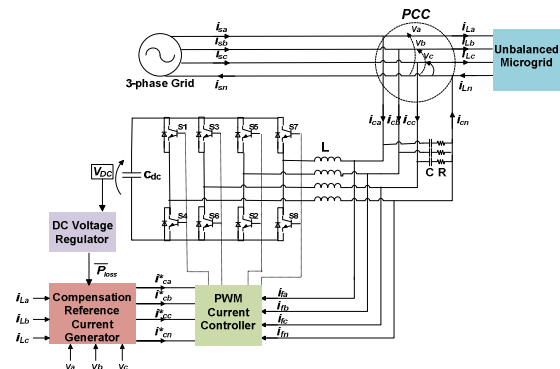


Fig. 7. Schematic of the Microgrid Unbalance Compensator

B. Compensation reference current generator

The compensation reference current generator is based on Instantaneous p-q Theory, which was first proposed in 1984 [18]. This utilizes an algebraic transformation known as the Clarke transformation. The 3-phase voltages and currents in the a-b-c coordinates are transformed into the $\alpha\beta 0$ coordinates by “(3)” where k represents ei-

ther voltage v or current i .

$$\begin{bmatrix} k_0 \\ k_\alpha \\ k_\beta \end{bmatrix} = \sqrt{\frac{2}{3}} \begin{bmatrix} \frac{1}{\sqrt{2}} & \frac{1}{\sqrt{2}} & \frac{1}{\sqrt{2}} \\ 1 & -\frac{1}{2} & -\frac{1}{2} \\ 0 & \frac{\sqrt{3}}{2} & -\frac{\sqrt{3}}{2} \end{bmatrix} \begin{bmatrix} k_a \\ k_b \\ k_c \end{bmatrix} \quad (3)$$

Then the instantaneous real power p , the imaginary power q and the zero-sequence power p_0 are calculated in the $\alpha\beta 0$ coordinates by “(4)” [19].

$$\begin{bmatrix} p_0 \\ p \\ q \end{bmatrix} = \begin{bmatrix} v_0 & 0 & 0 \\ 0 & v_\alpha & v_\beta \\ 0 & v_\beta & -v_\alpha \end{bmatrix} \begin{bmatrix} i_0 \\ i_\alpha \\ i_\beta \end{bmatrix} \quad (4)$$

The three newly defined instantaneous powers can be separated into their average and oscillating components.

- Instantaneous zero-sequence power: $p_0 = \bar{p}_0 + \tilde{p}_0$
- Instantaneous imaginary power: $q = \bar{q} + \tilde{q}$
- Instantaneous real power: $p = \bar{p} + \tilde{p}$

It should be noted that the instantaneous zero-sequence power can only exist if the three-phase voltages and currents are both unbalanced. The compensation reference current generator is able to selectively choose the undesirable instantaneous power components supplied by the source and calculate their respective currents. These currents in the $\alpha\beta 0$ reference frame are then transformed back to the a-b-c coordinates and sent to the current controller as reference currents, i_{ca}^* , i_{cb}^* , and i_{cc}^* . The reference current for the fourth leg of the VSC, i_{cn}^* is the negative sum of the 3-phase reference currents as “(5)”.

$$i_{cn}^* = -(i_{ca}^* + i_{cb}^* + i_{cc}^*) \quad (5)$$

There are two main strategies for compensating the unbalance in a Microgrid. The first is the “constant source instantaneous power strategy”, where the neutral current is compensated while ensuring constant active power is provided to the source even under unbalanced source voltage conditions. This strategy aims to provide optimal power flow to the source. The instantaneous power components that need compensating are \tilde{p} , q and \tilde{p}_0 . The compensation of the neutral current is achieved by compensating the zero sequence current i_0 . The calculation of the compensating currents in the $\alpha\beta 0$ reference frame is given by “(6)”.

$$\begin{bmatrix} i_{c\alpha}^* \\ i_{c\beta}^* \\ i_{c0}^* \end{bmatrix} = \frac{1}{v_\alpha^2 + v_\beta^2} \begin{bmatrix} v_\alpha & v_\beta & 0 \\ v_\beta & -v_\alpha & 0 \\ 0 & 0 & v_\alpha^2 + v_\beta^2 \end{bmatrix} \begin{bmatrix} -\tilde{p} + \bar{p}_0 \\ -q \\ -i_0 \end{bmatrix} \quad (6)$$

The second is the “sinusoidal source currents strategy”, which compensates the neutral current while ensuring sinusoidal and balanced currents are provided to the source even under unbalanced source voltage conditions. The sinusoidal source currents strategy utilizes a positive sequence detector to detect the fundamental positive sequence voltage components ($v'_{+\alpha}$ and $v'_{+\beta}$), which replaces the original phase voltages as inputs to the reference current generator. The positive sequence detector allows the MUC to compensate all the components that differ from the fundamental positive-sequence current, leaving the main grid to supply this component only. Equation (7) shows the calculation of the reference currents [20].

$$\begin{bmatrix} i_{c\alpha}^* \\ i_{c\beta}^* \\ i_{c0}^* \end{bmatrix} = \frac{1}{v'_{+\alpha} + v'_{+\beta}} \begin{bmatrix} v'_{+\alpha} & v'_{+\beta} & 0 \\ v'_{+\beta} & -v'_{+\alpha} & 0 \\ 0 & 0 & v'_{+\alpha} + v'_{+\beta} \end{bmatrix} \begin{bmatrix} -\tilde{p} + \bar{p}_0 \\ -q \\ -i_0 \end{bmatrix} \quad (7)$$

Simulations of the two strategies were carried out in the Matlab/Simulink environment using the SimPowerSystem toolbox. The 3 phase system voltages and the load currents are unbalanced as can be seen from Fig. 8. The PWM VSC is modeled as an ideal controlled current source with power losses neglected.

The resulting unbalanced three phase source voltages (v_{sa}, v_{sb}, v_{sc}) and the load currents (i_{La}, i_{Lb}, i_{Lc}) are shown in Fig. 8 (a) and (b), respectively. Fig. 8(b) also shows the neutral current, i_{Ln} flowing due to the unbalanced loads. Under the “constant source instantaneous power strategy”, the simulation results show that the MUC is capable of compensating all the undesirable power components in the Microgrid, thus providing constant power flow to the main grid as well as compensating the imaginary power, as shown in Fig. 9(c). It also effectively compensates the neutral current but the resulting compensated source currents are no longer sinusoidal and unbalanced. Fig. 10, (e) and (f) show the simulation results when applying the “sinusoidal source currents strategy”. As the results show the compensated source currents are indeed sinusoidal and balanced and the neutral current is also effectively compensated, as shown in Fig. 10 (f). However, the active power flow is oscillatory and there remains a flow of imaginary power. The selection of the reference current generator strategy will depend on the compensation objective of the MUC.

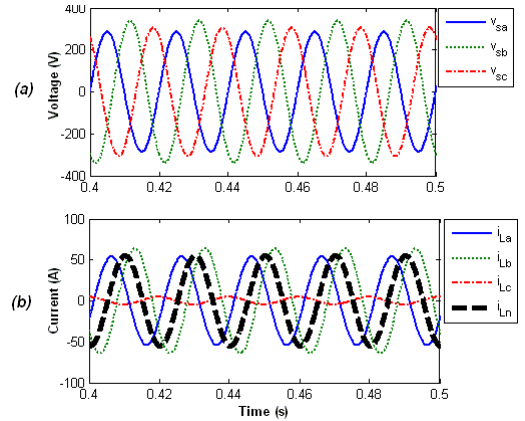


Fig. 8. Unbalanced source voltage and unbalanced load current.

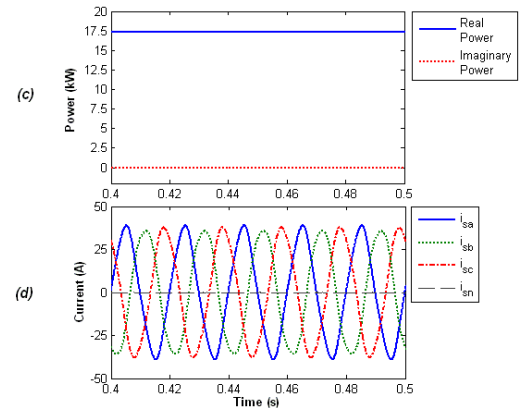


Fig. 9. Simulation results of “constant source instantaneous power strategy”.

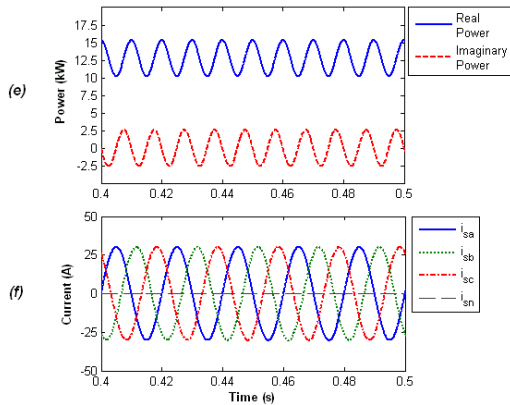


Fig. 10. Simulation results of "sinusoidal source currents strategy"

VII. CONCLUSION

A 300kW microgrid test facility is being developed in order to investigate management and control algorithms and equipment designed to operate in microgrid scenarios.

A wind turbine has been developed in order to capture actual wind and power generation data and at the same time data from a residential community is being collected.

Attached to the microgrid facility are emulator systems which represent energy generation and loads. The emulators use data taken in real-time from the wind turbine and/or CEH residential community to duplicate actual conditions. The emulators can however use modified data e.g. through models, to scale generation

The microgrid is currently being used to investigate community energy management algorithms such as the use of dispatchable energy resources.

A microgrid unbalance compensator is also being developed to improve power quality at the point of connection to the energy community.

VII. ACKNOWLEDGEMENTS

This work was supported by European Regional Development Fund (ERDF), within the Accelerating Low Carbon Economy (ALCE) project.

VIII. REFERENCES

- [1] European Wind Energy Association, "Wind energy and EU climate policy. Achieving 30% lower emissions by 2020," October 2011.
- [2] RenewableUK, "Small and Medium Wind. UK Market report," April 2012
- [3] A. Gupta, D.K. Jain, S. Dahiya, "Some Investigations on Recent Advances in Wind Energy Conversion Systems," 2012 IACSIT Coimbatore Conferences, IPCSIT vol. 28 (2012) IACSIT Press, Singapore
- [4] Dragomir, D. Golovanov, N. Postolache, P. Toader, C. , "The connection to the grid of wind turbines," PowerTech, 2009 IEEE Bucharest, pp.1-8, June 28 2009-July 2 2009
- [5] Eto, J. Lasseter, R. Schenkman, B. Stevens, J. Klapp, D. Volkommer, H. Linton, E. Hurtado, H. Roy, J., "Overview of the CERTS Microgrid laboratory Test Bed," Integration of Wide-Scale Renewable Resources Into the Power Delivery System, 2009 CIGRE/IEEE PES Joint Symposium , vol., no., pp.1, 29-31 July 2009
- [6] Hatziargyriou, N. Asano, H. Iravani, R. Marnay, C, "Microgrids," Power and Energy Magazine, IEEE , vol.5, no.4, pp.78-94, July-Aug. 2007
- [7] N.W.A. Lidula, A.D. Rajapakse, "Microgrids research: A review of experimental microgrids and test systems," Renewable and Sustainable Energy Reviews, Volume 15, Issue 1, January 2011, Pages 186-202.
- [8] University of Nottingham, "Creative Energy Homes," [Online] Available: <http://www.nottingham.ac.uk/creative-energy-homes/creative-energy-homes.aspx>
- [9] Davies, R, Sumner, M, Christophper, E, "The Development of Real-Time Wind Turbine Emulation for Microgrid Research" presented at the 15th EPE-PEMC 2012 ECCE Europe, 2012
- [10] A. Fazeli , Sumner, M, Johnson, C M, Christopher, E., "Coordinated Optimal Dispatch of Distributed Energy Resources within a Smart Energy Com-munity Cell," presented at the 2012 3rd IEEE PES Innovative Smart Grid Technologies Europe Berlin, 2012.
- [11] I. Richardson, M. Thomson, D. Infield, and C. Clifford, "Domestic electricity use: A high-resolution energy demand model," *Energy and Buildings*, vol. 42, pp. 1878-1887, 2010.
- [12] P. S. Anca D.Hansen, Lars H. Hansen and Henrik Bindner, "Models for a Stand-Alone PV System," Riso National Laboratory, Roskilde December 2000.
- [13] Miller, N.W.; Sanchez-Gasca, J.J.; Price, W.W.; Delmerico, R.W.; , "Dynamic modeling of GE 1.5 and 3.6 MW wind turbine-generators for stability simulations," Power Engineering Society General Meeting, 2003, IEEE , vol.3, no., pp. 1977- 1983 Vol. 3, 13-17 July 2003
- [14] WhisperGen, "WhisperGen™ (MkVb) microCHP System Design Manual,"2007. [Online] Available: http://www.whispergen.com/content/library/WP503703000_UK_USER1.pdf
- [15] R. X. a. J. F. Hongwen He *, "Evaluation of Lithium-Ion Battery Equivalent Circuit Models for State of Charge Estimation by an Experimental Approach," *Energies*, vol. 4, 2011.
- [16] D. Sreenivasarao, P. Agarwal and B. Das, "Neutral current compensation in three-phase, four-wire systems: A review", *Electric Power Systems Research*, Vol. 86, 2012, pp. 170-180.
- [17] A. Jouanne and B. Banerjee, "Assessment of Voltage Unbalance", *IEEE Transactions on Power Delivery*, Vol.16, No. 4, October 2001, pp. 782-790.
- [18] H. Akagi, Y. Kanazawa, and A. Nabae, "Instantaneous reactive power compensator comprising switching devices without energy storage components," *IEEE Trans. Ind. Appl.*, vol. IA-20, no. 3, pp. 625-630, 1984.
- [19] M. Aredes and E. H. Watanabe, "New control algorithms for series and shunt three-phase four-wire active power filters," *IEEE Trans. Power Delivery*, vol. 10, pp. 1649-1656, July 1995.
- [20] M. Aredes, H. Akagi, E. H. Watanabe, E. V. Salgado and L. F. Encarnação, "Comparisons Between the p-q and p-q-r Theories in Three-Phase Four-Wire Systems," *IEEE Trans. Power Electron.*, vol. 24, no. 4, pp. 924-933, April 2009.